Inorg. Chem. **2008**, *47*, 10037−10045

Computational Study of Iron Bis(dithiolene) Complexes: Redox Non-Innocent Ligands and Antiferromagnetic Coupling

Heiko Jacobsen*,† and James P. Donahue‡

KemKom, 1215 Ursulines Avenue, New Orleans, Louisiana 70116, and Department of Chemistry, Tulane University, 6400 Freret Street, New Orleans, Louisiana 70118

Received July 8, 2008

The molecular and electronic structure of monomeric ($[Fe(S_2C_2H_2)_2]^z$, $[Fe(S_2C_2(C_6H_4\text{-}p\text{-}OCH_3)_2)_2]^z$) and dimeric ($[\{Fe(S_2C_2H_2)_2\}_2]^z$) iron bis(dithiolene) complexes, and of their phosphine adducts ($[(PH_3)Fe(S_2C_2H_2)_2]^z$, $[(P(C_6H_5)_3)Fe(S_2C_2H_2)_2]^z$, $[(PH_3)Fe(S_2C_2(C_6H_4\text{-}p\text{-}OCH_3)_2)_2]^z$), carrying various charges ($z = 0, 1-, 2-$), have been investigated by density functional theory (DFT). Net total spin polarization values S of zero, two, and four have been considered for all neutral model compounds and their dianions, whereas all monoanions have been examined with net total spin polarization values S of one, three, and five. The DFT calculations utilized the pure functional BP86, as well as the hybrid functionals B3LYP and B3LYP*. For the monomers, the calculations reveal the presence of redox non-innocent dithiolene ligands and antiferromagnetic coupling between the ligands and the metal center. For the dimers, complexes with antiferromagnetically coupled iron centers have been found to represent structures of low energy, if not lowest energy structures. The spin-coupling constant of $[\{Fe(S_2C_2H_2)_2\}_2]^{2-}$ is calculated as $J = -230$ cm^{-1}. On the basis of the computational results, a model for reversible, electrochemically controlled binding and release of phosphine ligands to iron bis(dithiolene) complexes is proposed. Only BP86 and B3LYP* results, but not those of B3LYP calculations, are in qualitative agreement with experimental findings. BP86 calculations provide the best quantitative match in comparison with the experiment.

1. Introduction

Spawned by their remarkable set of properties, transition metal dithiolene complexes continue to be a focal point of ongoing research activities and of intense study for new materials and sensors.[1] Key to a detailed understanding of the properties of dithiolene complexes are their geometric as well as electronic structures.

Dithiolene ligands L in homoleptic bis(dithiolene) complexes ML_2 form relatively rigid and roughly planar five-membered rings, thus adopting a square-planar (SQ) coordination geometry. Owing to their electronic flexibility, some bis(dithiolene) structures build more expansive molecular arrangements. In particular, complexes of the d^8 and d^9 transition metals Fe and Co compose M−S type dimers of M_2L_4 stoichiometry.[2] The geometric arrangements of homoleptic dithiolene monomers and dimers are schematically

Scheme 1

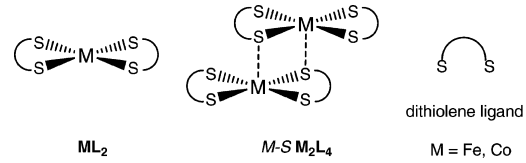

depicted in Scheme 1.

It has been recognized early on that monomeric as well as dimeric bis(dithiolene) complexes make up an extensive electron-transfer series as shown in Scheme 2.[3] It is this redox flexibility that is in large measure responsible for the properties and reactivity of this class of compounds, and Wieghardt and co-workers have investigated the electronic structure of monomeric[4,5] and dimeric[6] iron bis(dithiolene) complexes in much detail. The techniques employed included electronic absorption, infrared, X-band EPR, and Mössbauer spectroscopies as well as density functional theory (DFT)

* To whom correspondence should be addressed. E-mail: jacobsen@kemkom.com.
† KemKom.
‡ Tulane University.

(1) Stiefel, E. I. *Prog. Inorg. Chem.* **2004**, *52*, vii−ix.
(2) Beswick, C. L.; Schulman, J. M.; Stiefel, E. I. *Prog. Inorg. Chem.* **2004**, *52*, 55–110.
(3) Balch, A. L.; Dance, I. G.; Holm, R. H. *J. Am. Chem. Soc.* **1968**, *90*, 1139–1145.

10.1021/ic801277r CCC: $40.75
Published on Web 09/30/2008

Scheme 2

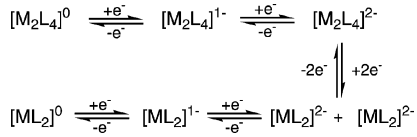

calculations, and they revealed redox non-innocent dithiolene ligands[5] and antiferromagnetically coupled iron centers.[6]

It is also well-known that monomeric bis(dithiolene) complexes of Fe and Co can extend their coordination sphere and accommodate a fifth ligand molecule,[7] and the coordination chemistry of ML_2 complexes continues to receive considerable attention.[8,9] We have recently reported the reversible, electrochemically controlled binding of phosphine to iron and cobalt bis(dithiolene) complexes,[10] a methodology that when paired with variation and tuning of the dithiolene ligand opens up the possibility to selectively bind various types of Lewis bases.

In this work, we present DFT calculations on monomers $[FeL_2]^z$, dimers $[Fe_2L_4]^z$, and phosphine adducts $[PR_3FeL_2]^z$ of dithiolene complexes with various charges, $z = 0, 1-, 2-$. Although a detailed density functional analysis has been presented for bis(dithiolene) complexes $[FeL_2]^{2-}$ and $[CoL_2]^-$,[4,11] dimeric complexes and phosphine adducts have not received the same computational attention. In particular, we want to address the issue of redox non-innocence of dithiolene ligands, antiferromagnetic coupling within dithiolene complexes, and the thermodynamics of charge-controlled phosphine binding. It is hoped that this computational study will assist the ongoing exploration of properties and potential applications of homoleptic bis(dithiolene) complexes. Knowledge of binding energies of Lewis bases to the metal−ligand framework of iron bis(dithiolene) complexes with different oxidation states of the central metal is of paramount importance for the design of a reversible, electrochemically controlled ligand binding scheme. Furthermore, detailed knowledge of the electronic structure assists in the spectroscopic identification of potentially active complexes. We note that reversible, electrochemically controlled ligand binding could find application in selective separations schemes, in the detection of specific molecules or molecule types, and in the storage or transportation of useful small molecules.[10]

After the initial success of DFT, it has become evident that a universal DFT method applicable to all problems in chemistry does not exist, and that it is advisable to evaluate different density functionals for any given problem. We thus begin not only with a brief outline, but also with a substantiation of our computational approach before discussing our results in more detail.

2. Computational Methodology

Gradient corrected density functional calculations were carried out with the Amsterdam Density Functional suite of programs, ADF version 2006.01.[12] Exchange is described by Slater's Xα potential,[13] with nonlocal corrections due to Becke.[14] Correlation is treated in the Vosko−Wilk−Nussair (VWN) parametrization using formula V,[15] with nonlocal corrections due to Perdew.[16] Orbitals are expanded in an uncontracted set of Slater-type orbitals. For H and C, the basis is of double-ζ quality, augmented with one set of polarization functions (ADF basis set DZP). The remaining elements are described with a triple-ζ basis, augmented by one set of polarization functions for S and P (ADF basis set TZP), and two sets of polarization functions for the transition metal (ADF basis set TZ2P). The core shells of carbon (1s), phosphorus (1s2s2p), sulfur (1s2s2p), and iron (1s2s2p) are treated by the frozen-core approximation.[17] Calculations on molecular systems utilized a numerical integration scheme that generates points and weights such that a large number of representative test integrals are evaluated with an accuracy of five significant digits. Unless stated otherwise, the calculations are unrestricted with an independent treatment of σ-spin densities ($\sigma = \alpha, \beta$). We designate different electronic states as *Sn*, the net total spin polarization, where *n* is the difference between the numbers of electrons with α and β spin, respectively. Closely related to (but distinct from) *Sn* is the atomic spin density, represented here as $S_\rho(X)$, at atom X. In calculations of the broken symmetry type, the use of molecular symmetry has been explicitly disabled, and adequate spin-polarized start-up potentials have been employed.

Geometries are optimized using the methodology developed by Versluis and Ziegler.[18] Frequency calculations utilize an analytical implementation of perturbations due to nuclear displacements.[19] Solvation is treated with an implementation of the conductor-like screening model,[20] as perturbative correction applied to gas-phase geometries.

(4) Ray, K.; Begum, A.; Weyhermüller, T.; Piligkos, S.; van Slageren, J.; Neese, F.; Wieghardt, K. *J. Am. Chem. Soc.* **2005**, *127*, 4403–4415.
(5) Ray, K.; Bill, E.; Weyhermüller, T.; Wieghardt, K. *J. Am. Chem. Soc.* **2005**, *127*, 5641–5654.
(6) Patra, A. K.; Bill, E.; Weyhermüller, T.; Stobie, K.; Bell, Z.; Ward, M. D.; McCleverty, J. A.; Wieghardt, K. *Inorg. Chem.* **2006**, *45*, 6541–6548.
(7) Balch, A. L. *Inorg. Chem.* **1967**, *6*, 2158–2162.
(8) Patra, A. K.; Bill, E.; Bothe, E.; Chlopek, K.; Neese, F.; Weyhermüller, T.; Stobie, K.; Ward, M. D.; McCleverty, J. A.; Wieghardt, K. *Inorg. Chem.* **2006**, *45*, 7877–7890.
(9) Ghosh, P.; Stobie, K.; Bill, E.; Bothe, E.; Weyhermüller, T.; Ward, M. D.; McCleverty, J. A.; Wieghardt, K. *Inorg. Chem.* **2007**, *46*, 522–532.
(10) Yu, R.; Arumugam, K.; Manepalli, A.; Tran, Y.; Schmehl, R.; Jacobsen, H.; Donahue, J. P. *Inorg. Chem.* **2007**, *46*, 5131–5133.
(11) Ray, K.; Petrenko, T.; Wieghardt, K.; Neese, F. *Dalton Trans.* **2007**, 1552–1566.
(12) (a) te Velde, G.; Bickelhaupt, F. M.; van Gisbergen, S. J. A.; Fonseca Guerra, C.; Baerends, E. J.; Snijders, J. G.; Ziegler, T. *J. Comput. Chem.* **2001**, *22*, 931–967. (b) Fonseca Guerra, C.; Snijders, J. G.; te Velde, G.; Baerends, E. J. *Theor. Chem. Acc.* **1998**, *99*, 391–403. (c) *ADF2006.01*; S.C.M., Theoretical Chemistry, Vrije Universiteit: Amsterdam, The Netherlands; http://www.scm.com.
(13) Slater, J. C. *Phys. Rev.* **1951**, *81*, 385–390.
(14) Becke, A. D. *Phys. Rev. A.* **1988**, *38*, 3098–3100.
(15) Vosko, S. H.; Wilk, L.; Nusair, M. *Can. J. Phys.* **1980**, *58*, 1200–1211.
(16) Perdew, J. P. *Phys. Rev. B.* **1986**, *33*, 8822–8824.
(17) Baerends, E. J.; Ellis, D. E.; Ros, P. *Chem. Phys.* **1973**, *2*, 41–51.
(18) Versluis, L.; Ziegler, T. *J. Chem. Phys.* **1988**, *88*, 322–328.
(19) (a) Wolff, S. K. *Int. J. Quantum Chem.* **2005**, *104*, 645–659. (b) Jacobsen, H.; Berces, A.; Swerhone, D. P.; Ziegler, T. *Comput. Phys. Commun.* **1997**, *100*, 263–276. (c) Berces, A.; Dickson, R. M.; Fan, L. Y.; Jacobsen, H.; Swerhone, D. P.; Ziegler, T. *Comput. Phys. Commun.* **1997**, *100*, 247–262. (d) Jacobsen, H.; Berces, A.; Swerhone, D. P.; Ziegler, T. *ACS Symp. Ser.* **1996**, *629*, 154–163.

Scheme 3

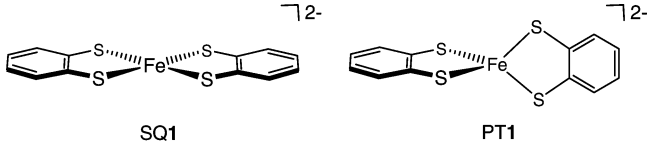

For molecular systems, total bond energies E have been calculated with reference to the constituting atomic fragments. To acquire enthalpy terms at 0 K, H^0, bond energy terms have been corrected for molecular zero-point energy contributions, obtained from frequency calculations. Free energy terms at 298 K, G^{298}, have been calculated from a thermal analysis of constituting thermodynamic properties.

2.1. Substantiation of the Methodology. Our computational approach used for geometry optimization and frequency calculation is commonly known as BP86, one of the first successful applications of DFT to transition metal complexes.[21] Exact exchange has been introduced into DFT by Becke,[22] which led to the development of so-called hybrid functionals. The B3LYP hybrid functional[23] by now has adopted the status of DFT-standard.

It is well-known from ab initio theory that, owing to the explicit consideration of Fermi correlation, exchange contributions favor states with largest values of the net total spin polarization S, that is the number of spin-α electrons in excess of spin-β electrons. Thus, when comparing pure and hybrid DFT methods, it turns out that a hybrid functional such as B3LYP stabilizes the high-spin states, whereas a pure DFT functional such as BP86 favors the low-spin states. This led to a reparameterization of the B3LYP functional based on energy differences of states with different multiplicities, and the modified functional is dubbed B3LYP*.[24] Because a series of iron−sulfur complexes served as a test set for the reparameterization,[24,25] B3LYP* would appear to be a suitable approach for the systems under investigation.

The quest for the most appropriate density functional in computational modeling of transition metal complexes continues to be an area of ongoing research activities.[26] Special attention has been given to the performance of pure density functionals in comparison with hybrid methods, and for certain systems, these two methodologies not only yield quantitatively, but also qualitatively different results.[27] To obtain a reliable description of transition-metal compounds, DFT calculations must not only produce the qualitatively correct ground-state net total spin polarization, but must also predict which one of the possible geometric isomers is of lowest energy. We have chosen the iron bis(dithiolene) complex $[Fe(S_2C_6H_4)_2]^{2-}$ **1** as a test case for our computational approach, and employed the BP86 functional to optimize the SQ as well as pseudotetrahedral (PT) geometries, Scheme 3.

In addition, we used the B3LYP and B3LYP* hybrid functionals in single-point energy calculations. We note as a technical detail that in hybrid calculations the frozen core approximation was not used, and the corresponding all-electron basis was chosen instead.

Table 1. Relative Bond Energies and Bond Enthalpies at 0 K[a], Obtained from BP86, B3LYP*, and B3LYP Calculations

	BP86		B3LYP*	B3LYP
	ΔH^0	ΔE	ΔE	ΔE
S0-SQ**1**	48	49	139	153
S2-SQ**1**	0	0	0	0
S4-SQ**1**	65	68	24	18
S0-PT**1**	66	67	131	153
S2-PT**1**	70	67	77	80
S4-PT**1**	38	38	15	−12

[a] In kJ/mol, with reference to *S2*-SQ**1** for *Sn*-SQ**1** and *Sn*-PT**1** (n = 0, 2, 4).

Wieghardt and Neese have studied the molecular and electronic structure of the iron bis(dithiolene) complex $[Fe(S_2C_6H_4)_2]^{2-}$ **1** in much detail.[4] A crystal structure analysis revealed that **1** adopts a SQ geometry; electronic structure calculations resulted in an intermediate-spin Fe(II) center with a spin density S_ρ(Fe) of 1.92. We can compare our test-case calculations with the work of Wieghardt and Neese,[4] and our results are collected in Table 1.

Both the BP86 as well as the B3LYP* calculations identify *S2*-SQ**1** as the lowest energy geometry, consistent with the work of Wieghardt and Neese.[4] The B3LYP functional, on the other hand, not only fails to reproduce the ground-state spin density but also the ground-state geometry; B3LYP calculations predict *S4*-PT**1** to represent the ground-state structure for the iron bis(dithiolene) complex **1**. We conclude that within the framework of the chosen computational engine, a program that utilizes Slater-type basis functions and numerical integration throughout, the hybrid functional B3LYP is not suitable to assess ground-state geometries of iron bis(dithiolene) complexes.

BP86 and B3LYP* calculations result in qualitatively similar descriptions of compound **1**. The complex at lowest energy in both cases is *S2*-SQ**1**, followed by *S4*-PT**1** in energetic ranking. As expected, the hybrid functional favors high-spin states whereas pure DFT stabilizes low spin-states. The energetic ranking for the SQ complexes from BP86 calculations is *S2*-SQ**1** < *S0*-SQ**1** < *S4*-SQ**1**, whereas B3LYP* calculations result in *S2*-SQ**1** < *S4*-SQ**1** < *S0*-SQ**1**. Similarly, for the PT geometries we find an energy scaling of *S4*-PT**1** < *S0*-PT**1** ≈ *S2*-PT**1** and *S4*-PT**1** < *S2*-PT**1** < *S0*-PT**1** from the BP86 and B3LYP* calculations, respectively. Nevertheless, both functionals not only predict the SQ geometry to be favored over a PT arrangement, but they also predict the same electronic ground state for both isomers SQ**1** and PT**1**. We conclude that our chosen computational approach should result in a consistent picture of the electronic structure of iron bis(dithiolene) complexes. It has been found before that the B3LYP* functional is in better qualitative agreement with pure density functionals,[28] and we expect that the calculations presented in this work present a qualitatively correct description for the model systems under investigation.

3. Results and Discussion

In the spirit of conceptual DFT,[29] we have investigated the molecular and electronic structure of monomeric $[Fe(S_2C_2H_2)_2]^z$ **2^z**, phosphine adducts $[(PH_3)Fe(S_2C_2H_2)_2]^z$ **3^z**, and dimeric $[\{Fe(S_2C_2H_2)_2\}_2]^z$ **4^z** iron bis(dithiolene) model compounds and anions, z = 0, 1−, 2−, Scheme 4.

Net total spin polarization values *Sn* with n = zero, two, and four have been considered for all neutral model

(20) Pye, C. C.; Ziegler, T. *Theor. Chem. Acc.* **1999**, *101*, 396–408.
(21) Ziegler, T. *Chem. Rev.* **1991**, *91*, 651–667.
(22) (a) Becke, A. D. *J. Chem. Phys.* **1993**, *98*, 1372–1377. (b) Becke, A. D. *J. Chem. Phys.* **1993**, *98*, 5648–5652.
(23) Stephens, P. J.; Devlin, F. J.; Chabalowski, C. F.; Frisch, M. J. *J. Phys. Chem.* **1994**, *98*, 11623–11627.
(24) Reiher, M.; Salomon, O.; Hess, B. A. *Theor. Chem. Acc.* **2001**, *107*, 48–55.
(25) Reiher, M. *Inorg. Chem.* **2002**, *41*, 6928–6935.
(26) Furche, F.; Perdew, J. P. *J. Chem. Phys.* **2006**, *124*, 044103.
(27) Cavallo, L.; Jacobsen, H. *J. Phys. Chem. A* **2003**, *107*, 5466–5471.
(28) Jacobsen, H.; Cavallo, L. *Phys. Chem. Chem. Phys.* **2004**, *6*, 3747–3753.
(29) Geerlings, P.; De Proft, F.; Langenaeker, W. *Chem. Rev.* **2003**, *103*, 1793–1873.

Scheme 4

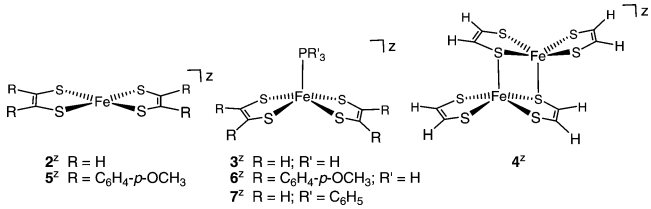

compounds and their dianions, whereas all monoanions have been examined with net total spin polarization values *Sn* with n = one, three, and five. Furthermore, the scope of the calculations has been broadened by including the extended real monomeric complex $[Fe(S_2C_2(C_6H_4\text{-}p\text{-}OCH_3)_2)_2]^z$ **5z** and its phosphine adduct $[(PH_3)Fe(S_2C_2(C_6H_4\text{-}p\text{-}OCH_3)_2)_2]^z$ **6z**, as well as the triphenylphosphine model complex $[(P(C_6H_5)_3)Fe(S_2C_2H_2)_2]^z$ **7z**.

3.1. Monomeric Model Compounds: Redox Non-Innocent Ligands. Hybrid as well as pure DFT methods predict that for model **2z**, independent of its charge z, an electronic state with two or three unpaired electrons represents the state at lowest energy. Thus, the ground-state systems are *S2*-$\mathbf{2}^0$, *S3*-$\mathbf{2}^{1-}$, and *S2*-$\mathbf{2}^{2-}$, and we shall discuss their electronic structures in terms of atomic charges and atomic spin densities. Out of the many charge models that are currently used in computational chemistry, we have chosen Hirshfeld charges q,[30] which use bonded-atom fragments for describing molecular charge densities. Contrary to the popular Mulliken charges, which often are useless because of heavy basis set dependency, it has been demonstrated that the Hirshfeld analysis yields chemically meaningful charges.[31] Spin densities, S_ρ, have been obtained from a dipole preserving multipole-derived charge analysis,[32] which best reproduces the electrostatic potential around a molecule. We will use these models for charge and spin throughout our work. Results of our analysis are collected in Table 2.

Comparing the Hirshfeld charges at iron q(Fe) of the neutral species *S2*-$\mathbf{2}^0$ with that of the monoanion *S3*-$\mathbf{2}^{1-}$, it appears that the iron center does not significantly change its charge value upon reduction. On the other hand, the sulfur atoms and the CH groups gain a substantial amount of negative charge when an electron is added to the system. This trend continues when going from the monoanion to the dianion.

Only for the dianion *S2*-$\mathbf{2}^{2-}$ does the value of the spin density at iron, S_ρ(Fe), suggest that the complex possesses a true triplet ground state with two unpaired electrons located at the transition metal center. This conclusion is based on the spin density value being close to the integer value of two. For the neutral complex and the monoanion, spin delocalization between the transition metal and dithiolene ligands occurs and results in antiferromagnetic and ferromagnetic ligand−metal coupling for *S2*-$\mathbf{2}^0$ and *S3*-$\mathbf{2}^{1-}$, respectively.

The non-innocent nature of dithiolene ligands with respect to redox chemistry has long been recognized, and electron-transfer series of bis(dithiolene) complexes continue to receive considerable attention.[33] Our calculations corroborate the notion of a redox non-innocent ligand. The results of Table 2 indicate that one-electron reduction of an iron bis(dithiolene) system such as *S2*-**2** is a ligand-based event. The dithiolene ligand gains a substantial amount of negative charge compared to the metal center.

The electronic structure of $[Fe(S_2C_6H_4)_2]^{2-}$ **1** has been investigated in detail by Wieghardt and Neese,[4] and we present only a brief exemplary analysis of the frontier orbital composition of compound *S0*-$\mathbf{2}^0$, Figure 1. To simplify the qualitative orbital analysis, we not only chose an *S0*-complex with no net total spin polarization, but we also performed spin restricted calculations.

We point out that Figure 1 is intended only to present a pictorial representation of major contributions to relevant orbitals and to assist in developing an intuitive picture of the active orbital manifold of iron bis(dithiolene) complexes. An *S0* state does not properly describe the multiplet electronic states that are present in many of the complexes under investigation because the frontier orbital characters differ as the number of unpaired electrons changes. Furthermore, the orbital picture for the *S2*-$\mathbf{2}^0$, *S3*-$\mathbf{2}^{1-}$, and *S2*-$\mathbf{2}^{2-}$ ground-state structures is more complex because of the independent α- and β-charge densities. However, the basic qualitative trends and observation drawn from an analysis of the *S0*-$\mathbf{2}^0$ orbital manifold are also valid for the true ground-state electronic structure. We refer the interested reader to the Supporting Information, Figure S1, which displays a frontier orbital scheme for compounds *S2*-$\mathbf{2}^0$, *S3*-$\mathbf{2}^{1-}$, and *S2*-$\mathbf{2}^{2-}$.

Four relevant orbitals among the set of active frontier orbitals are displayed in Figure 1. The major contribution to the highest occupied molecular orbital (HOMO) $1b_{3g}$ comes from a metal d-orbital with minor antibonding contributions from the four dithiolene sulfur atoms. The lowest unoccupied molecular orbital (LUMO) $2a_g$ constitutes a metal d-orbital that extends perpendicular to the plane of the ligand. These two orbitals are close in energy (ΔE < 0.1 eV), which suggests that the groundstate of $\mathbf{2}^0$ possesses at least two unpaired electrons. The HOMO-1 $1b_{1u}$ is a ligand based orbital without any metal contributions and comprises portions of the extended π-system of the dithiolene ligands. The LUMO+1 $2b_g$ again is ligand based but carries antibonding contributions from a metal d-orbital.

It is the set of these four orbitals that is actively involved in redox behavior and coordination chemistry of iron bis(dithiolene) complexes. For instance, the excitation from *S3*-$\mathbf{2}^{1-}$, the calculated ground-state structure of the monoanion, to *S1*-$\mathbf{2}^{1-}$, requires a change in the net total spin polarization and involves an electronic transition from the metal−ligand antibonding orbital $2b_{2g}$, the HOMO among the set of α-orbitals, into the metal based $2a_g$ orbital, the

(30) Hirshfeld, F. L. *Theor. Chim. Acta* **1977**, *44*, 129–138.
(31) Fonseca Guerra, C.; Handgraaf, J. W.; Baerends, E. J.; Bickelhaupt, F. M. *J. Comput. Chem.* **2004**, *25*, 189–210.
(32) Swart, M.; van Duijnen, P. T.; Snijders, J. G. *J. Comput. Chem.* **2001**, *22*, 79–88.
(33) Fomitchev, D. V.; Lim, B. S.; Holm, R. H. *Inorg. Chem.* **2001**, *40*, 645–654.

Table 2. Hirshfeld Charges q and Spin Densities, S_ρ, Summed over Ligand Groups, for Iron Bis(dithiolene) Complexes of Varying Charge and Net Total Spin Polarization, Sn,[a] Obtained from BP86 and B3LYP* Calculations

		q(Fe)	q(S)	q(CH)	S_ρ(Fe)	ΣS_ρ(S)	ΣS_ρ(CH)
BP86	*S2*-**2**^{0}	0.0601	0.0084	−0.0235	2.38	−0.28	−0.12
	S3-**2**$^{1-}$	0.0236	−0.1368	−0.1191	2.68	0.20	0.12
	S2-**2**$^{2-}$	−0.1905	−0.2526	−0.1998	1.95	0.00	0.05
B3LYP*	*S2*-**2**^{0}	0.0864	−0.0092	−0.0124	2.56	−0.40	−0.14
	S3-**2**$^{1-}$	0.0611	−0.1572	−0.1081	2.74	0.28	0.08
	S2-**2**$^{2-}$	−0.1437	−0.2781	−0.1859	2.01	−0.05	0.04

[a] n is the difference between the numbers of electrons with α and β spin, respectively.

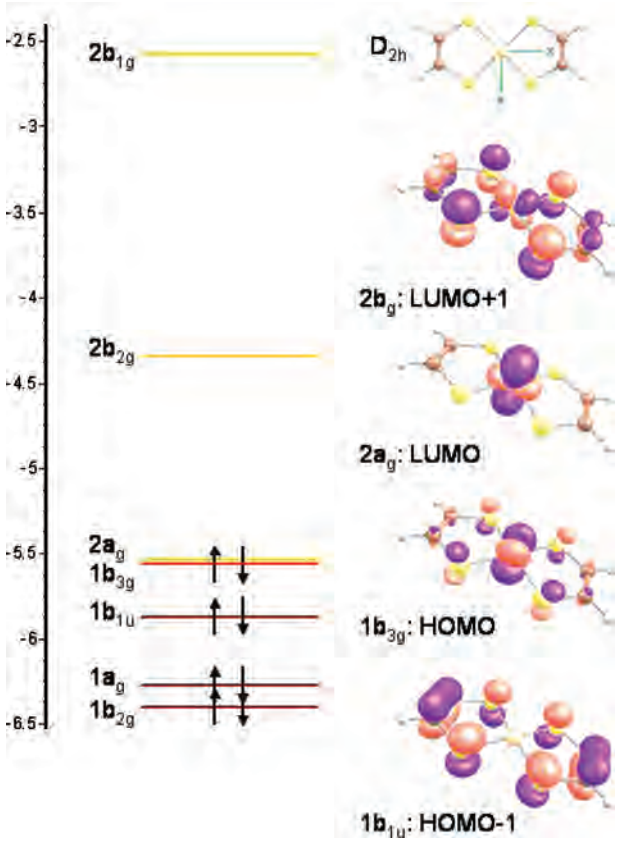

Figure 1. Frontier orbital diagram (energies in eV) from restricted BP86 calculations and representative Kohn−Sham MO orbitals (contour value = 0.05 au) of *S0*-**2**^{0}.

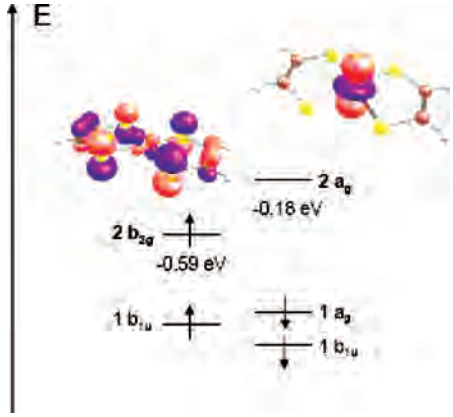

Figure 2. Frontier orbital diagram from unrestricted BP86 calculations and representative Kohn−Sham MO orbitals (contour value = 0.05 au) of *S3*-**2**$^{1-}$.

LUMO among the set of β-orbitals. Figure 2 illustrates the set of representative frontier orbitals for *S3*-**2**$^{1-}$.

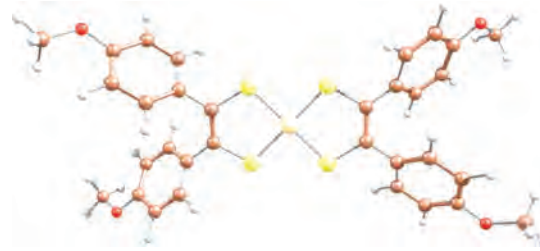

Figure 3. Optimized BP86 geometry of *S3*-**5**$^{1-}$.

Table 3. Bond Distances d (in pm), Spin Density S_ρ, and Relative Energies ΔE (in kJ/mol) for Monoanionic Iron Bis(dithiolene) Complexes, Obtained from BP86 Calculations

	S3-**2**$^{1-}$	*S1*-**2**$^{1-}$	*S3*-**5**$^{1-}$	*S1*-**5**$^{1-}$	X-ray[a]
d(Fe−S)	223	220	221	217	218
d(C$_S$−C$_S$)[b]	135	136	137	138	137
S_ρ(Fe)	2.68	1.38	2.55	1.30	
ΣS_ρ(S)	0.20	−0.32	0.27	−0.26	
ΔE	0	7	0	7	

[a] Crystal structure of $[Fe(S_2C_2(C_6H_4$-p-$OCH_3)_2)_2]^{1-}$, ref 10. [b] C$_S$: dithiolene carbon atom.

As a consequence, this transition is accompanied not only by an increase in energy of about 25 kJ/mol but also by a decrease of the Fe−S bond length.

We have determined the crystal structure of $[Fe(S_2C_2(C_6H_4$-p-$OCH_3)_2)_2]^{1-}$,[10] and we use the results for the monoanionic iron bis(dithiolene) complexes **2**$^{1-}$ and **5**$^{1-}$ to assess the reliability of our calculations in comparison with experimental results, and to evaluate the performance of our simplified model system. An exemplary optimized BP86 geometry of *S3*-**5**$^{1-}$ is displayed in Figure 3; bond distances, net total spin polarizations, and relative energies are collected in Table 3.

The data of the model compound **2**$^{1-}$ compare well with those of the real molecule **5**$^{1-}$. Bond distances are within 3 pm, and the model compound **2**$^{1-}$ displays somewhat longer distances. However, the trend that structures with a net total spin polarization $S = 3$ form longer Fe−S bonds than those with $S = 1$ is consistently observed for the model compound **2**$^{1-}$ and the real molecule **5**$^{1-}$. Furthermore, for both compounds **2**$^{1-}$ and **5**$^{1-}$ it is calculated that the energy difference between the *S1* and *S3* states amounts to only 7 kJ/mol. Such a small energy difference approaches the limit of computational reliability and should be interpreted with care. If we, for instance, compare the calculated bond lengths of **5**$^{1-}$ with those of $[Fe(S_2C_2(C_6H_4$-p-$OCH_3)_2)_2]^{1-}$ in the crystal, it appears that the calculated geometry of *S1*-**5**$^{1-}$, although not the geometry at lowest energy, provides a better match with the data obtained from X-ray analysis.

It is gratifying to notice that one of the computed structures shows an excellent agreement with the crystal structure.

Table 4. Relative Energies ΔE and Phosphine Dissociation Enthalpies (in kJ/mol), as well as Fe−P Bond Lengths (in pm) for Phosphine Adducts of Monomeric Iron Bis(dithiolene) Complexes

	S0-$\mathbf{3}^0$	*S2*-$\mathbf{3}^0$	*S1*-$\mathbf{3}^{1-}$	*S0*-$\mathbf{6}^0$	*S2*-$\mathbf{6}^0$	*S0*-$\mathbf{7}^0$	*S2*-$\mathbf{7}^0$	*S0*-$\mathbf{7}^{1-}$	X-ray[b]
ΔE	0	46		0	43	0	38		
ΔH_{diss}[a]	126	34	41	151	29	137	53	54	
d(Fe−P)	214	220	210	213	220	219	228	214	223

[a] ZPE corrections for complexes **6** and **7** taken from the corresponding electronic state of model compound **3**. [b] Data for [$(Ph_3P)Fe(S_2C_2(C_6H_4$-*p*-$OCH_3)_2)_2$], ref 10.

However, the small energetic difference is of the order where secondary effects might play a decisive role. It might be, for example, envisioned that the more compact geometric arrangement of the complex with shorter Fe−S separations lends itself to a more efficient 3D packing in the solid state.

What the data of Table 3 further show is the antiferromagnetic nature of the *S1* complexes. Both the iron center and the sulfur atoms show significant spin densities, but with opposite sign, indicating a surplus of α- and β-electron density, respectively. We also note that predicted trends in geometry based on qualitative orbital considerations are verified by the results of our geometry optimizations.

3.2. Phosphine Adducts. We have explored the potential of monomeric bis(dithiolene) complexes of iron to accommodate a fifth ligand molecule, and optimized geometries for a variety of phosphine adducts $\mathbf{3}^{\mathbf{z}}$, $\mathbf{6}^{\mathbf{z}}$, and $\mathbf{7}^{\mathbf{z}}$, $z = 0, 1-, 2-$. Main results for spin states of complexes, for which frequency calculations of model compounds resulted in a vibrational spectrum without any imaginary frequencies, are collected in Table 4.

For all neutral model complexes, the calculations reveal that the most stable state for phosphine adducts is the *S0*-state with no unpaired electrons. The spin-conserving phosphine dissociation enthalpy ΔH_{diss} for the neutral *S0* model compound *S0*-$\mathbf{3}^0$ is calculated as 126 kJ/mol and provides an estimate for the Fe−P bond strength. If we compare the H_3P complex of the model compound *S0*-$\mathbf{3}^0$ with that of the real molecule *S0*-$\mathbf{6}^0$, we observe an increase in ΔH_{diss} of about 25 kJ/mol. Further, if we compare H_3P and Ph_3P adducts of the model compound, *S0*-$\mathbf{3}^0$ and *S0*-$\mathbf{7}^0$, we find that the triphenyl phosphine adduct, which is often used in experimental studies, is more strongly bonded by about 10 kJ/mol. These results allow us to estimate a window of computational reliability of about 35 kJ/mol for phosphine bonding energies obtained from model compounds.

When we compare phosphine dissociation enthalpies from *S0* and *S2* states, we find that the Fe−P bond is significantly weaker in the *S2* states. At the same time, the Fe−P bond length increases by about 6 to 9 pm. The orbital picture presented in Figure 1 provides a qualitative explanation for this finding. The orbital responsible for formation of a donor−acceptor bond is the orbital $2a_g$. For *S2*-$\mathbf{2}^0$, the β-orbital of the $2a_g$ orbital set is unoccupied and available for bond formation, whereas the α-orbital holds one electron (see Supporting Information, Figure S1). Constructing a simplified picture, the lone pair of the phosphine ligand can engage only in half a P → Fe bond. On the other hand, if we analyze the orbitals for *S0*-$\mathbf{2}^0$, we find that that the complete spin-set of orbital $2a_g$ is unoccupied and available for bonding. This provides an explanation for the fact the ground state of the neutral phosphine adducts is the *S0* state, and that the Fe−P bonds are significantly stronger in the *S0* state than in the *S2* state.

For the different spin-states of the monoanion $\mathbf{2}^{\mathbf{1}-}$, an orbital analysis reveals that the set of orbitals $2a_g$ is at least partially occupied. We thus can expect that phosphine adducts of $\mathbf{2}^{\mathbf{1}-}$ are only weakly bonded. The data of Table 4 confirm this assumption, and the phosphine dissociation enthalpies ΔH_{diss} of *S2*-$\mathbf{3}^0$ and *S1*-$\mathbf{3}^{\mathbf{1}-}$ are of comparable size. At the same time, the Fe−P distance for *S1*-$\mathbf{3}^{\mathbf{1}-}$ *decreases* when compared to that of the most stable adduct *S0*-$\mathbf{3}^0$. It appears that the model compounds studied provide another example for the breakdown of bond length-bond strength correlation.[34,35] Without going into a detailed discussion, we note that besides orbital interaction, there are other decisive interactions that contribute to the energy of a chemical bond,[36] namely, Pauli repulsion and attractive electrostatic interactions. It is the latter contribution that causes a bond contraction upon moving from the charge-neutral model compound *S0*-$\mathbf{3}^0$ to the monoanion *S1*-$\mathbf{3}^{\mathbf{1}-}$.

When we compare optimized Fe−P bond lengths with crystal structure results of [$(Ph_3P)Fe(S_2C_2(C_6H_4$-*p*-$OCH_3)_2)_2$],[10] we can expect that model compound $\mathbf{7}^0$ should provide the best match. We also can expect that the Fe−P bond distance of $\mathbf{7}^0$ provides a lower limit to the bond length; the additional *p*-anisyl groups cause an increase in Pauli repulsion that corresponds to the intuitive concept of steric repulsion,[37] and one can reasonably expect an elongation of the Fe−P bond. The calculated Fe−P bond length of *S0*-$\mathbf{7}^0$ is 4 pm *shorter* than the one of [$(Ph_3P)Fe(S_2C_2(C_6H_4$-*p*-$OCH_3)_2)_2$], which is an acceptable agreement. On the contrary, the Fe−P separation in *S2*-$\mathbf{7}^0$ is 5 pm *longer* than for the real molecule, which is a highly unlikely situation. We conclude that the crystal structure of [$(Ph_3P)Fe(S_2C_2$-$(C_6H_4$-*p*-$OCH_3)_2)_2$] is in agreement with data for the *S0*, but not for the *S2* model compound, which confirms our computational results that the ground-state structure of phosphine adducts is represented by an *S0*-complex.

3.3. Dimeric Model Compounds: Antiferromagnetically Coupled Iron Centers. We have investigated various spin states of dimeric model compounds $\mathbf{4}^{\mathbf{z}}$, $z = 0, 1-, 2-$. Besides complexes with ferromagnetically coupled iron centers, we also optimized the geometry of complexes in which the two iron centers are antiferromagnetically coupled. In this case, both iron centers are spin-polarized but in terms of opposing spin-densities. We followed a broken-symmetry approach and used the methodology developed by Noodleman,[38] who also applied this method to a variety of iron−sulfur compounds.[39] For the charge neutral systems and the dianions, the net total spin polarization of the

(34) Kaupp, M.; Metz, B.; Stoll, H. *Angew. Chem., Int. Ed.* **2000**, *39*, 4607–4609.
(35) Jacobsen, H.; Fink, M. J. *Inorg. Chim. Acta* **2007**, *360*, 3511–3517.
(36) Jacobsen, H.; Ziegler, T. *Comments Inorg. Chem.* **1995**, *17*, 301–317.
(37) (a) Rosa, A.; Ricciardi, G.; Baerends, E. J. *J. Chem. Phys. A* **2006**, *110*, 5180–5190. (b) van den Hoek, P. J.; Kleyn, A. W.; Baerends, E. J. *Comments At. Mol. Phys.* **1989**, *23*, 93–110.
(38) Noodleman, L. *J. Chem. Phys.* **1981**, *74*, 5737–5743.

Table 5. Relative Energies (in kJ/mol) with Reference to the Antiferromagnetically Coupled System, and Spin Densities for Dimeric Model Compounds **4**, Obtained from BP86//BP86 and B3LYP*//BP86 Calculations

	BP86			B3LYP*		
	ΔE	S_ρ(Fe1)	S_ρ(Fe2)	ΔE	S_ρ(Fe1)	S_ρ(Fe2)
*S*0b-$\mathbf{4}^{0}$	0	1.48	−1.48	0	1.90	−1.90
*S*0-$\mathbf{4}^{0}$	32	0.00	0.00	64	0.00	0.00
*S*2-$\mathbf{4}^{0}$	−1	0.91	0.91	23	1.57	1.57
*S*4-$\mathbf{4}^{0}$	23	1.69	1.69	−2	2.08	2.08
*S*1b-$\mathbf{4}^{1-}$	0	1.50	−0.74	0	2.29	1.63
*S*1-$\mathbf{4}^{1-}$	8	0.45	0.45	38	0.80	0.80
*S*3-$\mathbf{4}^{1-}$	−15	1.22	1.22	9	1.54	1.54
*S*5-$\mathbf{4}^{1-}$	14	1.94	1.94	−17	2.21	2.21
*S*0b-$\mathbf{4}^{2-}$	0	2.20	−2.20	0	2.47	−2.47
*S*0-$\mathbf{4}^{2-}$	44	0.00	0.00	195	0.00	0.00
*S*2-$\mathbf{4}^{2-}$	33	1.08	1.08	122	1.18	1.18
*S*4-$\mathbf{4}^{2-}$	17	1.52	1.52	76	1.75	1.75

antiferromagnetically coupled complexes is zero, whereas for the anions it amounts to $S = 1$. We refer to these complexes as *S0b*-$\mathbf{4}^{0}$, *S1b*-$\mathbf{4}^{1-}$, and *S0b*-$\mathbf{4}^{2-}$, respectively, with a reference to broken-symmetry calculations. Results for dimeric model compounds are collected in Table 5.

We also report results from B3LYP* single-point calculations of BP86 geometries. Our methodology follows the computational scheme employed by Wieghardt and Neese,[4] who optimized geometries with a pure DFT method, and used hybrid functionals for property calculations.

Whereas for the monomeric complexes both BP86 as well as B3LYP* computations produce a qualitatively consistent picture, we observe significant differences for the dimeric compounds. For the dianion $\mathbf{4}^{2-}$, both approaches predict the antiferromagnetic system *S0b*-$\mathbf{4}^{2-}$ to represent the state at lowest energy. For the neutral system $\mathbf{4}^{0}$, both density functionals suggest that the antiferromagnetic state is in close energetic proximity (about 1 to 2 kJ/mol) to the ground state. However, whereas the BP86 approach favors the *S2*-$\mathbf{4}^{0}$ system, B3LYP* calculations put *S4*-$\mathbf{4}^{0}$ at lowest energy. This observation follows the expected trend that the hybrid functional favors high-spin states whereas pure DFT stabilizes low spin-states. The trend continues when we consider the monoanion $\mathbf{4}^{1-}$. The antiferromagnetically coupled complex *S1b*-$\mathbf{4}^{1-}$ is 15−17 kJ/mol higher in energy than the ground state, which according to BP86 calculations is the intermediate-spin complex *S3*-$\mathbf{4}^{1-}$, and according the B3LYP* calculations is the high-spin complex *S5*-$\mathbf{4}^{1-}$.

We evaluate the quality of our calculations in a comparison of optimized geometries with that of the solid state structure of $[Fe(S_2C_2(C_6H_4\text{-}p\text{-}OCH_3)_2]_2$.[10] Geometric data for the Fe_2S_2-core of various spin-state geometries of $\mathbf{4}^{0}$ together with data from an X-ray analysis are collected in Figure 4.

The optimized geometries of *S0b*-$\mathbf{4}^{0}$ and *S2*-$\mathbf{4}^{0}$ are very similar; bond distances of the Fe_2S_2-core differ by about 1 pm, and the angles of the Fe_2S_2-rhombus are within a deviation of less than one degree. The larger angle of 104°

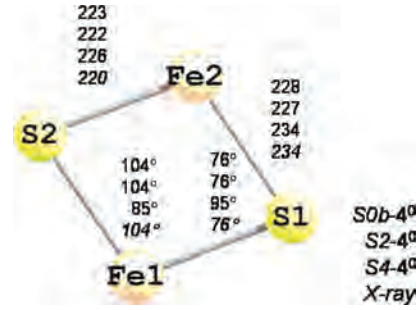

Figure 4. Bond distances (in pm) and bond angles of the Fe_2S_2-core of $\mathbf{4}^{0}$ from calculations of various spin-states and from X-ray analysis.

is found around iron, whereas the angle at sulfur is notably smaller with 76°. We recall that BP86 calculations put the *S0b*-$\mathbf{4}^{0}$ and *S2*-$\mathbf{4}^{0}$ states at almost identical energy. The *S4*-$\mathbf{4}^{0}$ geometry is significantly different: The acute angle of the Fe_2S_2-rhombus is now at the iron, and the obtuse angle is found around the sulfur.

The comparison of geometries of our model complexes *S0b*-$\mathbf{4}^{0}$, *S2*-$\mathbf{4}^{0}$, and *S4*-$\mathbf{4}^{0}$ with the solid state structure of $[Fe(S_2C_2(C_6H_4\text{-}p\text{-}OCH_3)_2)_2]_2$ is complicated by various effects. Crystal packing effects might substantially distort the molecular framework. We have recently found that the presence of a crystalline environment can overcome structural preferences for geometries energetically separated by about 20 kJ/mol.[40] We also have to keep in mind that the exemplary character of our model compounds prohibits an unbiased one-to-one comparison with the crystal structure.

Noodleman and Case have reported a geometry comparison of $[Fe_4S_4(SCH_3)_4]^{z-}$ ($z = 0, 1, 2, 3, 4$) model clusters optimized in BP86 calculations and crystal structures of synthetic analogs of the active sites of iron−sulfur proteins.[41] Deviations between theory and experiment in Fe−S* bond lengths, S* being a sulfur atom bridging two Fe atoms in the Fe_4S_4 cubane core, range from −8.5 pm to +5.5 pm. This study sets the stage of what accuracy can be expected from calculations of the type presented here. We estimate that our calculations should be able to reproduce the experimental value with an accuracy of ±7 pm. When we compare our optimized geometries with the crystal structure, it appears that in terms of Fe−S bond lengths, all three model complexes considered are in agreement with the experiment.

When we consider the angular geometry of the Fe_2S_2 rhombus, we see that the crystal structure displays obtuse angles ∠(S−Fe−S) and acute angles ∠(Fe−S−Fe). The optimized geometries of *S0b*-$\mathbf{4}^{0}$ and *S2*-$\mathbf{4}^{0}$ not only qualitatively but also quantitatively reproduce the angular geometry of the Fe_2S_2 rhombus. On the contrary, the geometry of *S4*-$\mathbf{4}^{0}$ is in qualitative disagreement with the experiment.

We also recall that the *S0b*-$\mathbf{4}^{0}$ and *S2*-$\mathbf{4}^{0}$ calculated structures are structures of lowest energy of model complex $\mathbf{4}^{0}$. It is most satisfying that the latter two structures, but not the calculated structure of *S4*-$\mathbf{4}^{0}$, present fair representations of the Fe_2S_2-core in the solid state.

(39) (a) Noodleman, L.; Baerends, E. J. *J. Am. Chem. Soc.* **1984**, *106*, 2316–2327. (b) Noodleman, L.; Norman, J. G.; Osborne, J. H.; Aizman, A.; Case, D. A. *J. Am. Chem. Soc.* **1985**, *107*, 3418–3426. (c) Noodleman, L.; Peng, C. Y.; Case, D. A.; Mouesca, J.-M. *Coord. Chem. Rev.* **1995**, *144*, 199–244.

(40) Jacobsen, H.; Fink, M. J. *Eur. J. Inorg. Chem.* **2007**, 5294–5299.

(41) Torres, R. A.; Lovell, T.; Noodleman, L.; Case, D. A. *J. Am. Chem. Soc.* **2003**, *125*, 1923–1936.

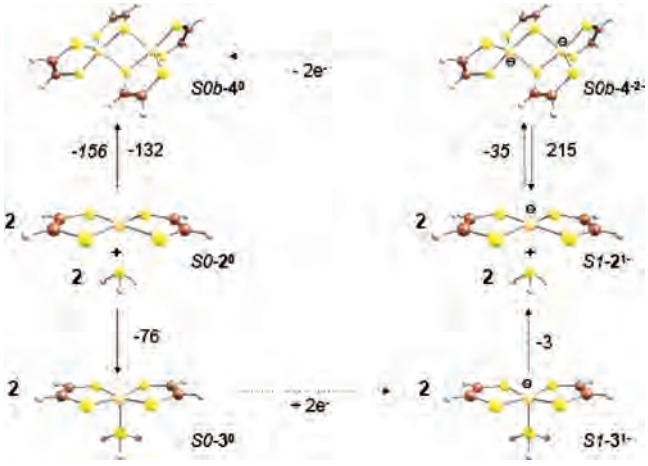

Figure 5. Free energies ΔG^{298} for dimerization and phosphine adduct formation for model compounds *S0*-$\mathbf{2}^0$ and *S1*-$\mathbf{2}^{\mathbf{-1}}$. Values shown in *italics* are corrected for solvation in dichloromethane.

Because the BP86 calculations disfavor the unlikely *S4*-$\mathbf{4}^0$ geometry, whereas B3LYP* calculations lean toward this questionable spin state geometry, it appears that the BP86 approach is more than an appropriate computational method for a proper description of iron bis(dithiolene) complexes. Because for the dianion $\mathbf{4}^{2-}$ both computational approaches unequivocally predict an *S0b* ground state with antiferromagnetically coupled iron centers, we also calculate the spin−spin coupling constant J for complex $\mathbf{4}^{2-}$, following the broken-symmetry methodology developed by Noodleman.[38] From BP86 calculations, we estimate a value of $J = -230$ cm^{-1}. This value is in good agreement with the experimentally determined spin-coupling of the related complex $[Fe_2(^1L)_4]^{2-}$ (^1L = $S_2C_2(C_6H_4$-*p*-$C(CH_3)_3)_2$), for which Mössbauer spectroscopic data revealed the presence of two equivalent iron centers that couple antiferromagnetically with $J = \sim -250$ cm^{-1}.[6] The B3LYP* calculations on the other hand result in a value of the spin-coupling constant that is more than four times as large, $J = -1060$ cm^{-1}. This result further corroborates our conclusion that the BP86 functional is most appropriate for computational studies of iron bis(dithiolene) dimers.

3.4. Electrochemically Controlled Reaction Pathways. With the data for monomers, dimers, and phosphine adducts at hand, we propose an oxidation/reduction-controlled reaction pathway for iron bis(dithiolene) complexes. The free energy profile for dissociation/association reactions at 298 K is presented in Figure 5. Both the dimerization and the phosphine adduct formation of *S0*-$\mathbf{2}^0$ are exergonic processes at room temperature. Solvation effects stabilize the dimeric complex *S0b*-$\mathbf{4}^0$ by about 35 kJ/mol. The data for the model compound indicate that dimerization is favored over phosphine adduct formation by about 75 kJ/mol. Referring back to the data presented in section 3.2, we can expect that for real molecules the Fe−P bond is stronger by at least 25 kJ/mol. At the same time, we anticipate that the energy for formation of the dimer would decrease. Thus, for real molecules, the processes of adduct formation and dimerization can be expected to be more compatible.

Upon reduction of the phosphine adduct *S0*-$\mathbf{3}^0$, the Fe−P bond is significantly weakened. As a consequence, the anion *S1*-$\mathbf{3}^{\mathbf{1}-}$ possesses no thermodynamic stability and dissociates into the monomeric anion *S1*-$\mathbf{2}^{\mathbf{1}-}$ and the free phosphine.

Because of the negative charge, the gas phase dimerization of *S1*-$\mathbf{2}^{\mathbf{1}-}$ constitutes an endergonic reaction. However, if solvation is included in the calculation, the formation of dimer of *S0b*-$\mathbf{4}^{\mathbf{2}-}$ turns into a thermodynamically favorable process. The free energy for product formation, 35 kJ/mol, is rather low. As a consequence, an equilibrium between monomeric anions and dimeric dianions is observed in the experiment.

Our calculations are in accord with experimental studies and support the mechanism of reversible, electrochemically controlled binding of phosphine to an iron bis(dithiolene) complex.[10]

4. Conclusion

The coordination chemistry and reactivity of dithiolene ligands is to a large part characterized by their non-innocent nature,[11] which determines not only their redox behavior but also the metal−ligand electronic interaction. Theoretical investigations continue to support an unambiguous assignment of the otherwise complicated electronic structure of transition metal complexes involving non-innocent ligands. In this study, we could substantiate the non-innocent redox behavior and an antiferromagnetic metal−ligand interaction of iron bis(dithiolene) monomers. We also were able to provide theoretical support for antiferromagnetically coupled iron-centers of iron bis(dithiolene) dimers. Our computational results allow us to propose an oxidation/reduction-controlled reaction pathway for binding and release of phosphine ligands by iron bis(dithiolene) complexes. A set of four orbitals is actively involved in redox behavior and coordination chemistry of iron bis(dithiolene) complexes, which allows one to construct qualitative predictions of the reactivity of iron bis(dithiolene) complexes. Our findings support ongoing studies that utilize dithiolene ligand modulations to provide a basis for selectivity for the type of Lewis base adduct formed by iron bis(dithiolene) complexes.

The computational engine that is routinely used to provide theoretical support for investigations of transition metal complexes is DFT, now a common computational chemistry tool to examine a broad variety of structures and reactions involving increasingly larger molecules. However, there is growing and convincing evidence that not all density functional methods provide satisfying agreement with experimental results, and among those is the most popular B3LYP functional, which often is considered as the standard of DFT. It has been stated that "the happy days of black box DFT usage are over, at least for energy evaluations".[42] When carrying out calculations of transition metal complexes, it is advisable to evaluate various DFT approaches, and our calculations indicate that for calculations of iron bis(dithiolene) complexes, pure

density functional approaches perform substantially better than hybrid methodologies.

Acknowledgment. KemKom acknowledges Prof. L. Cavallo for granting access to the MoLNaC computing facilities at Dipartimento di Chimica, Università di Salerno. J.P.D. thanks the Petroleum Research Fund (Award # 545884G1) and Tulane University for financial support of this research.

Supporting Information Available: Frontier orbital diagram of *S2*-$\mathbf{2}^{0}$, *S3*-$\mathbf{2}^{1-}$, *S2*-$\mathbf{2}^{2-}$. Cartesian coordinates, total bond energies, zero-point energies, entropic terms, spin-densities, and lowest frequencies for all optimized structures. This material is available free of charge via the Internet at http://pubs.acs.org.

IC801277R

(42) Schreiner, P. R. *Angew. Chem., Int. Ed.* **2007**, *46*, 4217–4219.